

# ***CD36* identified by weighted gene co-expression network analysis as a hub candidate gene in lupus nephritis**

Huiying Yang<sup>1</sup>, Hua Li<sup>Corresp. 1</sup>

<sup>1</sup> Department of Nephrology, Sir Run Run Shaw Hospital, Zhejiang University School of Medicine, Hangzhou, Zhejiang Province, China

Corresponding Author: Hua Li  
Email address: h\_li@zju.edu.cn

Lupus nephritis (LN) is a severe manifestation of systemic lupus erythematosus (SLE), which often progresses to end-stage renal disease (ESRD) and ultimately leads to death. At present, there are no definitive therapies towards LN, so that illuminating the molecular mechanism behind the disease has become an urgent task for researchers. Bioinformatics has become a widely utilized method for exploring genes related to disease. This study set out to conduct weighted gene co-expression network analysis (WGCNA) and screen the hub gene of LN. We performed WGCNA on the microarray expression profile dataset of GSE104948 from Gene Expression Omnibus (GEO) database with 18 normal and 21 LN samples of glomerulus. A total of 5,942 genes were divided into 5 co-expression modules, one of which was significantly correlated to LN. Gene Ontology (GO) and Kyoto Encyclopedia of Genes and Genomes (KEGG) enrichment analyses were conducted on the LN-related module and the module was proved to be associated mainly with the activation of inflammation, immune response, cytokines, and immune cells. Genes in the most significant GO terms were extracted for sub-networks of WGNCA. We evaluated the centrality of genes in the sub-networks by Maximal Clique Centrality (MCC) method and *CD36* was ultimately screened out as a hub candidate gene of the pathogenesis of LN. The result was verified by its differentially expressed level between normal and LN in GSE104948 and the other three multi-microarray datasets of GEO. Moreover, we further demonstrated that the expression level of *CD36* is related to the WHO Lupus Nephritis Class of LN patients with the help of Nephroseq database. The current study proposed *CD36* as a vital candidate gene in LN for the first time and *CD36* may perform as a brand-new biomarker or therapeutic target of LN in the future.

1  
2 **CD36 identified by weighted gene co-expression**  
3 **network analysis as a hub candidate gene in lupus**  
4 **nephritis**

5  
6  
7 Huiying Yang<sup>1</sup>, Hua Li<sup>1</sup>

8  
9 <sup>1</sup> Department of Nephrology, Sir Run Run Shaw Hospital, Zhejiang University School of  
10 Medicine, Hangzhou, China

11  
12 Corresponding Author:

13 Hua Li

14 3 Qingchun East Road, Hangzhou, Zhejiang province, China

15 Email address: h\_li@zju.edu.cn  
16

17 **Abstract**

18 Lupus nephritis (LN) is a severe manifestation of systemic lupus erythematosus (SLE), which  
19 often progresses to end-stage renal disease (ESRD) and ultimately leads to death. At present,  
20 there are no definitive therapies towards LN, so that illuminating the molecular mechanism  
21 behind the disease has become an urgent task for researchers. Bioinformatics has become a  
22 widely utilized method for exploring genes related to disease. This study set out to conduct  
23 weighted gene co-expression network analysis (WGCNA) and screen the hub gene of LN. We  
24 performed WGCNA on the microarray expression profile dataset of GSE104948 from Gene  
25 Expression Omnibus (GEO) database with 18 normal and 21 LN samples of glomerulus. A total  
26 of 5,942 genes were divided into 5 co-expression modules, one of which was significantly  
27 correlated to LN. Gene Ontology (GO) and Kyoto Encyclopedia of Genes and Genomes (KEGG)  
28 enrichment analyses were conducted on the LN-related module and the module was proved to be  
29 associated mainly with the activation of inflammation, immune response, cytokines, and immune  
30 cells. Genes in the most significant GO terms were extracted for sub-networks of WGCNA. We  
31 evaluated the centrality of genes in the sub-networks by Maximal Clique Centrality (MCC)  
32 method and *CD36* was ultimately screened out as a hub candidate gene of the pathogenesis of  
33 LN. The result was verified by its differentially expressed level between normal and LN in  
34 GSE104948 and the other three multi-microarray datasets of GEO. Moreover, we further  
35 demonstrated that the expression level of *CD36* is related to the WHO Lupus Nephritis Class of  
36 LN patients with the help of Nephroseq database. The current study proposed *CD36* as a vital  
37 candidate gene in LN for the first time and *CD36* may perform as a brand-new biomarker or  
38 therapeutic target of LN in the future.

## 39 Introduction

40 Systemic lupus erythematosus (SLE) is a chronic, systemic autoimmune disease characterized by  
41 autoantibody production, complement activation and immune complex deposition. The incidence  
42 of SLE ranges from 0.03‰ to 2.32‰ person-years worldwide (Rees et al. 2017).

43 Lupus nephritis (LN) is one of the most frequent and severe organ manifestations in patients with  
44 SLE, the hallmark of which is often glomerulonephritis. Approximately 50% of SLE patients  
45 develop clinically evident renal disease, up to 11% of whom develop end-stage renal disease  
46 (ESRD) at 5 years (Tektonidou, Dasgupta and Ward 2016, Almaani, Meara and Rovin 2017). LN  
47 is an important cause of ESRD and mortality. The initial and subsequent therapy of LN mainly  
48 consists of immunosuppressants and glucocorticoids, which means there are little efficient and  
49 specific therapies. Thus, it is a pressing task to clarify molecular mechanisms involved in LN.  
50 LN is characterized by its complicated physiopathologic mechanism. In LN patients, the  
51 formation of immune complexes in different glomerular compartments, the activation of innate  
52 immune signal pathways, the infiltration of immune cells and proinflammatory mediators can  
53 harm glomerular cells through various approaches (Devarapu et al. 2017). Although many  
54 studies have determined certain pathological mechanisms of LN, the pathogenesis is still far  
55 from clear.

56 With the development of gene microarray and high-throughput next-generation sequencing,  
57 bioinformatics analysis of gene expression profiling has been broadly applied to explore the  
58 mechanism underlying diseases and potential diagnostic biomarkers or treatment targets. Among  
59 diverse means aiming to investigate altered molecular elements based on comparison between  
60 groups of different states, weighted gene co-expression network analysis (WGCNA) is a  
61 powerful tool utilized for describing the correlation patterns among genes and exploring hub  
62 genes related to certain traits (van Dam et al. 2018, Langfelder and Horvath 2008). WGCNA  
63 constructs a co-expression network between genes, and then, genes are divided into several co-  
64 expression modules by clustering techniques. Genes in certain module are deemed to share  
65 similar biological function and biological process. At last, after relating modules to clinical traits,  
66 modules with high correlation to disease are further analyzed and hub genes of pivotal  
67 importance to disease are identified. WGCNA has been broadly used for studying of diseases  
68 such as cancer (Jardim-Perassi et al. 2019), neuropsychiatric disorder (Huggett and Stallings  
69 2019), chronic disease (Morrow et al. 2015) and proved to be quite useful.

70 However, although researchers have conducted numerous bioinformatics studies about LN and  
71 have got many achievements (Arazi et al. 2019, Panousis et al. 2019), WGCNA has rarely been  
72 used for studies of LN (Sun et al. 2019). In our study, we constructed a co-expression network of  
73 the expression profile of glomerulus tissue by WGCNA and confirmed gene modules related to  
74 LN. After systematically analyzing the LN-related co-expression module by series of  
75 bioinformatics methods, a hub gene associated with LN was identified and verified. Depend on  
76 the potential roles of the hub gene in the pathogenesis of LN, we expect to propose novel clues  
77 of the diagnosis and treatment of LN.

## 78 Materials & Methods

**79 Expression profile data collection**

80 The overall procedures of our study are illustrated in the flow chart (Fig. 1). The gene expression  
81 profile of GSE104948 was selected and obtained from the Gene Expression Omnibus (GEO)  
82 database (<https://www.ncbi.nlm.nih.gov/geo/>). The raw data is available in the GEO database.  
83 The dataset consists of microarray-based gene expression profiles of 32 LN samples and 18  
84 normal samples of glomerular tissues from SLE patients and living kidney transplant donors  
85 respectively. The glomerular tissues were microdissected and verified with glomerular-selective  
86 transcripts (Grayson et al. 2018). The expression values have already been log<sub>2</sub> transformed.

**87 Data preprocessing**

88 The probe annotation was conducted under the Perl environment with the microarray platform  
89 file. Probes matching with multiple genes were removed, and for genes corresponding to  
90 multiple probes, the average values of probes were regarded as the expression values of the  
91 genes. A total of 11,884 genes were left after the probe annotation.

92 Since non-varying genes are usually regarded as background noise, we filtered the genes by  
93 variance and the top 50% (5,942 genes) with larger variance were chosen for subsequent  
94 analyses.

**95 Weighted co-expression network construction and module division**

96 Before WGCNA, we excluded the outlier samples by sample clustering with the hierarchical  
97 clustering method. After that, we applied WGCNA with the expression profile by using the  
98 WGCNA package (Langfelder and Horvath 2008) in the R environment (version 3.5.3). Firstly,  
99 we calculated the Pearson's correlation for all pair-wise genes and constructed a correlation  
100 matrix. Secondly, the correlation matrix was transformed to an adjacency matrix (also known as  
101 scale-free network) with an appropriate soft-thresholding value  $\beta$ . A reasonable  $\beta$  value would  
102 emphasize strong correlations between genes and penalize weak ones. We calculated the scale-  
103 free fit index and mean connectivity of each  $\beta$  value from 1 to 30 respectively, and when the  
104 scale-free fit index is up to 0.85, the  $\beta$  value with highest mean connectivity is deemed as the  
105 most appropriate one. Then, the adjacency matrix was converted to a topological overlap matrix  
106 (TOM) so that the indirect correlations between genes are concerned. Finally, we used average  
107 linkage hierarchical clustering according to the TOM-based dissimilarity measure to classify all  
108 genes into several co-expression modules with a minimum size of 30 genes, thereby the genes  
109 with similar expression patterns were divided into the same module. After defining the first  
110 principal component of a given module as eigengene, we calculated the Pearson's correlations of  
111 the eigengenes, and merged modules whose eigengenes were highly correlated (with Pearson's  
112 correlation higher than 0.75) into one module.

113 To verify the reliability of the division of modules, we plotted an adjacency heatmap of all the  
114 5,942 genes analyzed by WGCNA. Besides, we completed a cluster analysis of module  
115 eigengenes and plotted an adjacency heatmap to find out the interactions among modules.

**116 Identification of clinically significant modules**

117 The clinical traits of our samples included normal and LN, we calculated the correlation between  
118 modules and traits. Modules of positive correlation with LN were considered as playing roles in

119 the pathogenesis of the disease. On the other hand, genes in modules of positive correlation with  
120 normal trait are indispensable for maintaining normal biological functions. Thus, we extracted  
121 gene modules of highest correlation with LN and normal for subsequent studies.  
122 Here, we introduced the definition of gene significance (GS) and module membership (MM),  
123 which represent the correlation of a given gene with clinical trait and module eigengene  
124 respectively. Genes in clinical-related modules should have high values and preferable  
125 correlations of GS and MM.

### 126 **GO and KEGG pathway enrichment analyses**

127 To explore the involved signal pathways and biological characteristics of genes in clinical-  
128 related modules, we conducted Gene Ontology (GO) enrichment analysis and Kyoto  
129 Encyclopedia of Genes and Genomes (KEGG) pathway enrichment analysis and visualized the  
130 top 10 significant terms respectively with the clusterProfiler R package (Yu et al. 2012). For both  
131 of GO and KEGG, enrichment terms arrived the cut-off criterion of  $p$ -value  $< 0.01$  and  
132 Benjamin-Hochberg adjusted  $p$ -value  $< 0.01$  were considered as significant ones.

### 133 **Differentially expressed genes analysis**

134 To investigate the difference of the expression profiles between normal and LN samples of genes  
135 in clinical-related modules, we applied differentially expressed genes (DEGs) analysis based on  
136 Empirical Bayes test with the limma R package (Ritchie et al. 2015). The cut-off criterion was  
137 set as follow:  $|\log_2\text{fold change (logFC)}| > 1$ ;  $p$ -value  $< 0.01$ ; false discovery rate ( $FDR$ )  $< 0.001$ .  
138 The results were visualized with the heatmap R package (Galili et al. 2018).

### 139 **Identification of hub gene**

140 Hub gene of the LN-related module should have high connectivity with the whole module and  
141 LN trait, which may play critical roles in the molecular mechanism of LN. For identifying the  
142 hub gene related with LN, we extracted gene clusters that enriched in certain GO terms from the  
143 WGCNA network to construct sub-networks after GO enrichment analysis of the LN-related  
144 module. Then, we utilized the Cytoscape software and its plug-in cytohubba to seek out the hub  
145 gene from sub-networks (Shannon et al. 2003). After calculating the Maximal Clique Centrality  
146 (MCC) value of each gene, those with high MCC values was regarded as hub genes (Chin et al.  
147 2014). The results were exhibited with the Cytoscape software. We then surveyed the GS value,  
148 MM value and logFC value of the selected hub gene to validate its reasonability.

### 149 **Validation of hub gene with the other GEO datasets**

150 To further verify the differential expression level of the hub gene between normal and LN  
151 tissues, we analyzed the logFC value of the hub gene with data from the other three GEO  
152 datasets (GSE32591, GSE99339 and GSE113342). The GEO IDs and details of the datasets were  
153 given in Table. S1.

### 154 **Validation of the clinical significance of hub gene by Nephroseq database**

155 To assess the relationship between the expression level of the hub gene and the activity or grade  
156 of LN, we visited the Nephroseq database (<http://v5.nephroseq.org>), which provides unique  
157 access to datasets from the Applied Systems Biology Core at the University of Michigan,  
158 incorporating clinical data which is often difficult to collect from public sources. We then

159 analyzed the difference of the expression level of hub gene between patients in different WHO  
160 Lupus Nephritis Class (Weening et al. 2004) based on two datasets (the dataset of Peterson  
161 Lupus Glom and the dataset of Berthier Lupus Glom) from Nephroseq database (details available  
162 in Supplemental Document. 1). We performed unpaired t test for comparisons between groups  
163 and set the criterion of two-tailed value of  $p < 0.05$  as statistically significant.

## 164 **Results**

### 165 **Data preprocessing**

166 After data preprocessing, 5,942 genes were selected for subsequent analyses. Sample clustering  
167 excluded the outlier samples and a total of 18 normal samples and 21 LN samples were left. The  
168 final result of sample clustering is shown in Fig. 2A, revealing satisfactory intra-group  
169 consistency and distinct difference between groups. The GEO IDs and details about the source of  
170 the samples are available in Table. S1.

### 171 **Weighted co-expression network construction and module division**

172 In the current study, taking both scale-free fit index and mean connectivity as reference, the soft-  
173 thresholding was determined as 10 (Fig. 2B and Fig. 2C). Accordingly, the correlation matrix  
174 was transformed to an adjacency matrix and then converted to a topological overlap matrix.  
175 Based on average linkage hierarchical clustering and module merging, the genes were divided  
176 into 6 modules and were displayed with different colors (Fig. 3A), including the black, blue,  
177 brown, magenta, pink, and grey modules, containing 220, 2,881, 777, 465, 770, and 829 genes,  
178 respectively. Genes in the grey module were those couldn't be divided into any co-expression  
179 modules.

180 Fig. 3B depicts the topological overlap adjacency among all the 5,942 genes analyzed by  
181 WGCNA, indicating that most genes have higher correlation with genes in the same module and  
182 lower correlation with genes in other modules, which means the division of the modules was  
183 accurate. The clustering dendrogram and adjacency heatmap of eigengene are shown in Fig. 3C  
184 and Fig. 3D, meaning that the 5 modules were mainly separated into two clusters.

### 185 **Identification of clinically significant modules**

186 We calculated the module-trait correlation coefficients and showed the results in Fig. 4A. The  
187 results illuminated that the blue module displayed highest correlation with LN trait ( $r = 0.91$ ,  $p =$   
188  $2e-15$ ), while the brown module related best with normal trait ( $r = 0.66$ ,  $p = 4e-06$ ). The GS and  
189 MM value of all member genes of the blue and brown modules were shown in the scatterplots  
190 (Fig. 4B and Fig. 4C). The GS and MM value were of high correlation in the two modules ( $cor =$   
191  $0.89$ ,  $p < 1e-200$ , and  $cor = 0.73$ ,  $p = 3.1e-130$  respectively), suggesting that the genes in the two  
192 modules were associate with their module eigengenes and clinical traits synchronously and thus  
193 suitable for further analyses and hub gene excavation. We then renamed the two modules as top  
194 LN module and top non-LN module respectively.

### 195 **DEGs analysis of trait-related modules**

196 We applied DEGs analysis for the two trait-related modules. For the top LN module, 203 DEGs  
197 were screened in LN compare with normal, including 195 up-regulated genes and 8 down-  
198 regulated ones. While, the top non-LN module contained 78 DEGs, all of which were down-

199 regulated. The top 30 of up-regulated and down-regulated genes are displayed in Fig. 5  
200 respectively. The logFC value,  $p$ -value, and  $FDR$  of DEGs are given in Table. S2.

### 201 **GO and KEGG Enrichment analyses of trait-related modules**

202 To confirm the biological themes of genes in the trait-related modules and find the underlying  
203 biological pathways behind LN, we performed GO and KEGG enrichment analyses towards the  
204 top LN and top non-LN modules and the top 10 significant terms of GO and KEGG are exhibited  
205 in Fig. 6 and Fig. 7 respectively. The complete results of GO and KEGG enrichment analyses  
206 were given in Table. S3.

207 For the top LN module, enriched GO-BP terms were mainly about activation of immune  
208 response, immune cells, cytokine production, and inflammation (Fig. 6A), such as “neutrophil  
209 activation” (gene count = 178,  $p = 7.26e-301.52E-20$ ), “positive regulation of defense response”  
210 (gene count = 160,  $p = 9.14e-25$ ), “activation of innate immune response” (gene count = 107,  $p =$   
211  $3.45e-18$ ). Enriched GO-MF terms were mainly about cytokine and their receptors (Fig. 6B),  
212 such as “cytokine binding” (gene count = 39,  $p = 2.47e-8$ ), “cytokine receptor activity” (gene  
213 count = 34,  $p = 5.3e-7$ ), “cytokine receptor binding” (gene count = 69,  $p = 2.98e-5$ ). For GO-CC,  
214 enriched terms were mainly involved in membrane and endocytic vesicle (Fig. 6C), such as  
215 “vesicle lumen” (gene count = 107,  $p = 4.13e-15$ ), “cytoplasmic vesicle lumen” (gene count =  
216 106,  $p = 8.99e-15$ ), “membrane region” (gene count = 95,  $p = 2.33e-12$ ). The results of KEGG  
217 enrichment were similar to that of GO-BP, were mainly about immune and inflammation (Fig.  
218 7A). The top KEGG terms included “Complement and coagulation cascades” (gene count = 31,  $p$   
219  $= 6.55e-6$ ), “Fc gamma R-mediated phagocytosis” (gene count = 34,  $p = 1.90e-5$ ), “Th1 and Th2  
220 cell differentiation” (gene count = 33,  $p = 3.05e-5$ ). Meanwhile, several well-known pathways  
221 involved in LN were also included, such as Th17 cell differentiation.

222 On the other hand, for the top non-LN module, the GO-BP results were mainly involved in the  
223 metabolism process of different kinds of molecule (Fig. 6D), for example, “small molecule  
224 catabolic process” (gene count = 93,  $p = 3.27e-41$ ), “organic acid catabolic process” (gene count  
225 = 73,  $p = 3.97e-39$ ), “carboxylic acid catabolic process” (gene count = 73,  $p = 3.97e-39$ ). The top  
226 10 terms of GO-MF and GO-CC are also displayed (Fig. 6E and Fig. 6F). Similarly, the top  
227 KEGG terms were mainly about metabolism process (Fig. 7B).

228 Besides, we found that the magenta module also had high correlation with LN trait. The results  
229 of enrichment analyses of magenta module are also given in Table. S3.

### 230 **Identification and validation of hub gene**

231 We extracted the genes enriched in two of the top 10 significant GO-BP terms in top LN module,  
232 namely “neutrophil activation” and “positive regulation of defense response”, and constructed  
233 two sub-networks of the weighted co-expression network respectively. Co-expression pairs with  
234 top 500 weighted correlations in the sub-networks were selected for hub gene excavation. After  
235 importing the gene co-expression pairs and their weighted correlations into Cytoscape, we  
236 calculated the MCC value of genes and the most central genes of the sub-network were screened  
237 out as shown in Fig. 8. In both sub-networks, *CD36* had the maximum MCC value among all,  
238 and was therefore deemed as the hub gene under the pathogenesis of LN.

239 The GS and MM value of *CD36* were 0.772 and 0.833, revealing *CD36* was significant  
240 correlated with the top LN module and LN trait. The DEGs analysis showed that the expression  
241 level of *CD36* in LN was abnormally up-regulated compared with that of normal. The logFC of  
242 *CD36* was 2.298, which ranked 11th among all.

#### 243 **Validation of hub gene with the other GEO datasets**

244 For verifying our conclusion in a broader range, we interrogated the GEO database for more  
245 datasets about LN. We downloaded the datasets of GSE32591, GSE99339 and GSE113342, and  
246 then analyzed the differentially expressed level of *CD36* between LN and normal (Fig. 9). In the  
247 four different datasets, the expression level of *CD36* was consistently up-regulated in LN  
248 samples, illustrating a satisfactory reliability of the result.

#### 249 **Validation of hub gene by Nephroseq database**

250 We analyzed the expression level of *CD36* in glomerular tissues under different severity of LN  
251 evaluated by WHO Lupus Nephritis Class. The result indicates that *CD36* was significantly up-  
252 regulated with the aggravation of LN (Fig. 10), that is to say, *CD36* plays an important role in  
253 the development of LN.

#### 254 **Discussion**

255 In the current study, we used the expression profile of GSE104948 to screen the hub gene  
256 involved in the pathogenesis of LN. We performed WGCNA and divided all genes into 5 co-  
257 expression modules. After relating the modules to clinical traits, we concluded that the blue  
258 module was of highest correlation with LN and was suitable for hub gene excavating. The brown  
259 module had the highest correlation with normal trait, and was also worthy of subsequent  
260 analyses. GO and KEGG enrichment illuminated that genes in the top LN module were mostly  
261 enriched in biological themes of the activation of inflammation, immune response, cytokine, and  
262 immune cells, and the top non-LN module was mainly about the metabolism process of various  
263 molecules. What's more, DEGs analysis showed that almost all DEGs in top LN module were  
264 abnormally up-regulated, revealing an aberrant activated stage of inflammation and immune  
265 response in LN. On the other hand, all DEGs in the top non-LN module were down-regulated,  
266 meaning a reduced ability of material metabolism in LN. To achieve the ultimately purpose of  
267 finding out the hub gene, we extracted genes enriched in the GO terms of "neutrophil activation"  
268 and "positive regulation of defense response" and constructed sub-networks accordingly. Base  
269 on the MCC method, *CD36* with maximum value of MCC in both sub-networks was regarded as  
270 the hub gene behind the pathogenesis of LN. We investigated the GS, MM and logFC of *CD36*  
271 and validated its importance. We interrogated the GEO database and got more datasets of LN,  
272 the obvious overexpression of *CD36* was therefore further verified. Moreover, the association  
273 between *CD36* and WHO Lupus Nephritis Class provides strong evidence that *CD36* is a hub  
274 gene in the pathogenesis of LN.

275 The *CD36* gene is located on band q11.2 of chromosome 7 (Fernandez-Ruiz et al. 1993). The  
276 protein encoded by *CD36* is a kind of transmembrane protein (also known as scavenger receptor  
277 B2) expresses on the surface of various kinds of cells. In the glomerulus of kidney, *CD36*  
278 expresses in podocyte (Hua et al. 2015), mesangial cells (Ruan et al. 1999) and interstitial

279 macrophages (Kennedy et al. 2013). Meanwhile, *CD36* expresses in immunity correlating cells  
280 such as monocytes and macrophages (Collot-Teixeira et al. 2007). With multiple ligands, *CD36*  
281 involves in complex biological process such as lipid homeostasis, immune response and cell  
282 apoptosis.

283 There are no relative reports concerning the direct relationship between *CD36* and LN. Our  
284 results have shown that *CD36* mainly participates in the function of neutrophil, such as  
285 “neutrophil activation”, “neutrophil activation involved in immune response”, “neutrophil  
286 degranulation”, “neutrophil mediated immunity”, as well as the activation of immune response,  
287 such as “positive regulation of defense response”, “positive regulation of innate immune  
288 response”, “innate immune response-activating signal transduction”, “positive regulation of  
289 immune effector process”. Base on the results, we conclude that *CD36* performs important  
290 functions in the pathogenesis and development of LN through affecting the function of  
291 neutrophil and innate immune response. Studies have proved that deposited immune complexes  
292 (IC) could activate complement and attract neutrophils and potentiate their responses, which will  
293 lead to intense glomerulonephritis, release protease and Reactive Oxygen Species (ROS), and  
294 give rise to kidney involvement of SLE (Tsuboi et al. 2008). Besides, IC-induced activation of  
295 neutrophils can lead to the formation of neutrophil extracellular traps (NETs), which can be  
296 pathogenic and promote the release of type I interferon (Garcia-Romo et al. 2011). *CD36* may  
297 candidate in the pathogenesis of LN by the above-mentioned pathways.

298 Numerous studies have shown that *CD36* participates in the pathogenesis of several kinds of  
299 chronic kidney disease (CKD).

300 It has long been known that chronic inflammation is an important segment of the progression of  
301 CKD. Studies have proved that the ligands signal via *CD36* to promote inflammatory response  
302 and the recruitment and activation of macrophage in the glomerulus (Kennedy et al. 2013). A  
303 report of LN showed that renal macrophage is associated with onset of nephritis and indicates  
304 poor prognosis (Bethunaickan et al. 2011). Meanwhile, oxidant stress plays a critical role in  
305 glomerular dysfunction. Along with chronic inflammation, *CD36* may facilitate the development  
306 of oxidant stress in LN (Hua et al. 2015, Kennedy et al. 2013, Aliou et al. 2016).

307 Podocyte is most susceptible to injury among the component of the glomerulus and its injury  
308 leads to glomerular dysfunction in various renal diseases including LN. Here, we determined that  
309 podocyte functional markers were down-regulated in LN glomerular tissue, including *WT1*  
310 ( $\log_{2}FC = -0.273$ ,  $p = 0.009$ ) and *NPHS1* ( $\log_{2}FC = -0.306$ ,  $p = 0.034$ ), indicating the fact of  
311 podocyte injury. It is reported that in primary nephrotic syndrome mouse, the overexpression of  
312 *CD36* in the podocyte promotes its apoptosis (Yang et al. 2018). There is probably similar  
313 pathogenesis in the progression of LN.

314 Ectopic lipid deposition in kidney may cause lipotoxicity and further affect the function of the  
315 kidney (Lin et al. 2019). *CD36* is a multifunctional protein function as a key molecule in the  
316 uptake of long-chain fatty acids, which is the main component of fatty acids uptake system in the  
317 kidney and plays a critical rule in the development of CKD (Gai et al. 2019). The expression  
318 level of *CD36* is higher in kidney with acute or chronic damage, and lipid disorders will

319 stimulate the up-regulation of *CD36*. Furthermore, *CD36* can promote the uptake of lipid from  
320 plasma to tissue (Hua et al. 2015, Lin et al. 2019, Nosadini and Tonolo 2011, Yang et al. 2017).  
321 Among our results, the top 10 GO terms of non-LN module includes two terms about lipid  
322 metabolism: fatty acid catabolic process ( $p = 8.03e-22$ ) and fatty acid metabolic process ( $p =$   
323  $2.62e-20$ ), implying that lipid disorders exist in the glomerular tissue, in which *CD36* may take  
324 part.

325 Regrettably, as most reports on the relationship between *CD36* and kidney diseases are about the  
326 disorders of kidney in metabolic diseases, there is no study about the role *CD36* plays in immune  
327 response, which is worthy of further study in LN.

## 328 **Conclusions**

329 In conclusion, through WGCNA and a series of comprehensive bioinformatics analyses, *CD36*  
330 was confirmed for the first time as a hub gene in the pathogenesis of LN. *CD36* is likely to  
331 become a new biomarker or therapeutic target of LN. Our work might provide a new insight for  
332 exploring the molecular mechanisms of LN.

## 333 **References**

- 334 Aliou, Y., M. C. Liao, X. P. Zhao, S. Y. Chang, I. Chenier, J. R. Ingelfinger & S. L. Zhang  
335 (2016) Post-weaning high-fat diet accelerates kidney injury, but not hypertension programmed  
336 by maternal diabetes. *Pediatr Res*, 79, 416-24.
- 337 Arazi, A., D. A. Rao, C. C. Berthier, A. Davidson, Y. Liu, P. J. Hoover, A. Chicoine, T. M.  
338 Eisenhaure, A. H. Jonsson, S. Li, D. J. Lieb, F. Zhang, K. Slowikowski, E. P. Browne, A. Noma,  
339 D. Sutherby, S. Steelman, D. E. Smilek, P. Tosta, W. Apruzzese, E. Massarotti, M. Dall'Era, M.  
340 Park, D. L. Kamen, R. A. Furie, F. Payan-Schober, W. F. Pendergraft, 3rd, E. A. McInnis, J. P.  
341 Buyon, M. A. Petri, C. Putterman, K. C. Kalunian, E. S. Woodle, J. A. Lederer, D. A. Hildeman,  
342 C. Nusbaum, S. Raychaudhuri, M. Kretzler, J. H. Anolik, M. B. Brenner, D. Wofsy, N. Hachohen  
343 & B. Diamond (2019) The immune cell landscape in kidneys of patients with lupus nephritis.  
344 *Nat Immunol*, 20, 902-914.
- 345 Almaani, S., A. Meara & B. H. Rovin (2017) Update on Lupus Nephritis. *Clin J Am Soc*  
346 *Nephrol*, 12, 825-835.
- 347 Bethunaickan, R., C. C. Berthier, M. Ramanujam, R. Sahu, W. Zhang, Y. Sun, E. P. Bottinger, L.  
348 Ivashkiv, M. Kretzler & A. Davidson (2011) A unique hybrid renal mononuclear phagocyte  
349 activation phenotype in murine systemic lupus erythematosus nephritis. *J Immunol*, 186, 4994-  
350 5003.
- 351 Chin, C. H., S. H. Chen, H. H. Wu, C. W. Ho, M. T. Ko & C. Y. Lin (2014) cytoHubba:  
352 identifying hub objects and sub-networks from complex interactome. *BMC Syst Biol*, 8 Suppl 4,  
353 S11.
- 354 Collot-Teixeira, S., J. Martin, C. McDermott-Roe, R. Poston & J. L. McGregor (2007) *CD36* and  
355 macrophages in atherosclerosis. *Cardiovasc Res*, 75, 468-77.
- 356 Devarapu, S. K., G. Lorenz, O. P. Kulkarni, H. J. Anders & S. R. Mulay (2017) Cellular and  
357 Molecular Mechanisms of Autoimmunity and Lupus Nephritis. *Int Rev Cell Mol Biol*, 332, 43-  
358 154.

- 359 Fernandez-Ruiz, E., A. L. Armesilla, F. Sanchez-Madrid & M. A. Vega (1993) Gene encoding  
360 the collagen type I and thrombospondin receptor CD36 is located on chromosome 7q11.2.  
361 *Genomics*, 17, 759-61.
- 362 Gai, Z., T. Wang, M. Visentin, G. A. Kullak-Ublick, X. Fu & Z. Wang (2019) Lipid  
363 Accumulation and Chronic Kidney Disease. *Nutrients*, 11.
- 364 Galili, T., A. O'Callaghan, J. Sidi & C. Sievert (2018) heatmaply: an R package for creating  
365 interactive cluster heatmaps for online publishing. *Bioinformatics*, 34, 1600-1602.
- 366 Garcia-Romo, G. S., S. Caielli, B. Vega, J. Connolly, F. Allantaz, Z. Xu, M. Punaro, J. Baisch,  
367 C. Guiducci, R. L. Coffman, F. J. Barrat, J. Banchereau & V. Pascual (2011) Netting neutrophils  
368 are major inducers of type I IFN production in pediatric systemic lupus erythematosus. *Sci*  
369 *Transl Med*, 3, 73ra20
- 370 Grayson, P. C., S. Eddy, J. N. Taroni, Y. L. Lightfoot, L. Mariani, H. Parikh, M. T.  
371 Lindenmeyer, W. Ju, C. S. Greene, B. Godfrey, C. D. Cohen, J. Krischer, M. Kretzler & P. A.  
372 Merkel (2018) Metabolic pathways and immunometabolism in rare kidney diseases. *Ann Rheum*  
373 *Dis*, 77, 1226-1233.
- 374 Hua, W., H. Z. Huang, L. T. Tan, J. M. Wan, H. B. Gui, L. Zhao, X. Z. Ruan, X. M. Chen & X.  
375 G. Du (2015) CD36 Mediated Fatty Acid-Induced Podocyte Apoptosis via Oxidative Stress.  
376 *PLoS One*, 10, e0127507.
- 377 Huggett, S. B. & M. C. Stallings (2019) Cocaine'omics: Genome-wide and transcriptome-wide  
378 analyses provide biological insight into cocaine use and dependence. *Addict Biol*.
- 379 Jardim-Perassi, B. V., P. A. Alexandre, N. M. Sonehara, R. de Paula-Junior, O. Reis Junior, H.  
380 Fukumasu, R. Chammas, L. L. Coutinho & D. Zuccari (2019) RNA-Seq transcriptome analysis  
381 shows anti-tumor actions of melatonin in a breast cancer xenograft model. *Sci Rep*, 9, 966.
- 382 Kennedy, D. J., Y. Chen, W. Huang, J. Viterna, J. Liu, K. Westfall, J. Tian, D. J. Bartlett, W. H.  
383 Tang, Z. Xie, J. I. Shapiro & R. L. Silverstein (2013) CD36 and Na/K-ATPase-alpha1 form a  
384 proinflammatory signaling loop in kidney. *Hypertension*, 61, 216-24.
- 385 Langfelder, P. & S. Horvath (2008) WGCNA: an R package for weighted correlation network  
386 analysis. *BMC Bioinformatics*, 9, 559.
- 387 Lin, Y. C., M. S. Wu, Y. F. Lin, C. R. Chen, C. Y. Chen, C. J. Chen, C. C. Shen, K. C. Chen &  
388 C. C. Peng (2019) Nifedipine Modulates Renal Lipogenesis via the AMPK-SREBP  
389 Transcriptional Pathway. *Int J Mol Sci*, 20.
- 390 Morrow, J. D., W. Qiu, D. Chhabra, S. I. Rennard, P. Belloni, A. Belousov, S. G. Pillai & C. P.  
391 Hersh (2015) Identifying a gene expression signature of frequent COPD exacerbations in  
392 peripheral blood using network methods. *BMC Med Genomics*, 8, 1.
- 393 Nosadini, R. & G. Tonolo (2011) Role of oxidized low density lipoproteins and free fatty acids  
394 in the pathogenesis of glomerulopathy and tubulointerstitial lesions in type 2 diabetes. *Nutr*  
395 *Metab Cardiovasc Dis*, 21, 79-85.
- 396 Panousis, N. I., G. K. Bertsias, H. Ongen, I. Gergianaki, M. G. Tektonidou, M. Trachana, L.  
397 Romano-Palumbo, D. Bielser, C. Howald, C. Pamfil, A. Fanouriakis, D. Kosmara, A. Repa, P.  
398 Sidiropoulos, E. T. Dermitzakis & D. T. Boumpas (2019) Combined genetic and transcriptome

399 analysis of patients with SLE: distinct, targetable signatures for susceptibility and severity. *Ann*  
400 *Rheum Dis*, 78, 1079-1089.

401 Rees, F., M. Doherty, M. J. Grainge, P. Lanyon & W. Zhang (2017) The worldwide incidence  
402 and prevalence of systemic lupus erythematosus: a systematic review of epidemiological studies.  
403 *Rheumatology (Oxford)*, 56, 1945-1961.

404 Ritchie, M. E., B. Phipson, D. Wu, Y. Hu, C. W. Law, W. Shi & G. K. Smyth (2015) limma  
405 powers differential expression analyses for RNA-sequencing and microarray studies. *Nucleic*  
406 *Acids Res*, 43, e47.

407 Ruan, X. Z., Z. Varghese, S. H. Powis & J. F. Moorhead (1999) Human mesangial cells express  
408 inducible macrophage scavenger receptor. *Kidney Int*, 56, 440-51.

409 Shannon, P., A. Markiel, O. Ozier, N. S. Baliga, J. T. Wang, D. Ramage, N. Amin, B.  
410 Schwikowski & T. Ideker (2003) Cytoscape: a software environment for integrated models of  
411 biomolecular interaction networks. *Genome Res*, 13, 2498-504.

412 Sun, G., P. Zhu, Y. Dai & W. Chen (2019) Bioinformatics Analysis of the Core Genes Related to  
413 Lupus Nephritis Through a Network and Pathway-Based Approach. *DNA Cell Biol*, 38, 639-  
414 650.

415 Tektonidou, M. G., A. Dasgupta & M. M. Ward (2016) Risk of End-Stage Renal Disease in  
416 Patients With Lupus Nephritis, 1971-2015: A Systematic Review and Bayesian Meta-Analysis.  
417 *Arthritis Rheumatol*, 68, 1432-41.

418 Tsuboi, N., K. Asano, M. Lauterbach & T. N. Mayadas (2008) Human neutrophil Fcγ3  
419 receptors initiate and play specialized nonredundant roles in antibody-mediated inflammatory  
420 diseases. *Immunity*, 28, 833-46.

421 van Dam, S., U. Vosa, A. van der Graaf, L. Franke & J. P. de Magalhaes (2018) Gene co-  
422 expression analysis for functional classification and gene-disease predictions. *Brief Bioinform*,  
423 19, 575-592.

424 Weening, J. J., V. D. D'Agati, M. M. Schwartz, S. V. Seshan, C. E. Alpers, G. B. Appel, J. E.  
425 Balow, J. A. Bruijn, T. Cook, F. Ferrario, A. B. Fogo, E. M. Ginzler, L. Hebert, G. Hill, P. Hill,  
426 J. C. Jennette, N. C. Kong, P. Lesavre, M. Lockshin, L. M. Looi, H. Makino, L. A. Moura & M.  
427 Nagata (2004) The classification of glomerulonephritis in systemic lupus erythematosus  
428 revisited. *J Am Soc Nephrol*, 15, 241-50.

429 Weening, J. J., V. D. D'Agati, M. M. Schwartz, S. V. Seshan, C. E. Alpers, G. B. Appel, J. E.  
430 Balow, J. A. Bruijn, T. Cook, F. Ferrario, A. B. Fogo, E. M. Ginzler, L. Hebert, G. Hill, P. Hill,  
431 J. C. Jennette, N. C. Kong, P. Lesavre, M. Lockshin, L. M. Looi, H. Makino, L. A. Moura & M.  
432 Nagata (2004) The classification of glomerulonephritis in systemic lupus erythematosus  
433 revisited. *J Am Soc Nephrol*, 15, 241-50.

434 Yang, X., D. M. Okamura, X. Lu, Y. Chen, J. Moorhead, Z. Varghese & X. Z. Ruan (2017)  
435 CD36 in chronic kidney disease: novel insights and therapeutic opportunities. *Nat Rev Nephrol*,  
436 13, 769-781.

- 437 Yang, X., Y. Wu, Q. Li, G. Zhang, M. Wang, H. Yang & Q. Li (2018) CD36 Promotes Podocyte  
438 Apoptosis by Activating the Pyrin Domain-Containing-3 (NLRP3) Inflammasome in Primary  
439 Nephrotic Syndrome. *Med Sci Monit*, 24, 6832-6839.
- 440 Yu, G., L. G. Wang, Y. Han & Q. Y. He (2012) clusterProfiler: an R package for comparing  
441 biological themes among gene clusters. *Omics*, 16, 284-7.

# Figure 1

Flow chart of the whole procedures in this study.

Data processing, analyses, hub gene identification and validation.

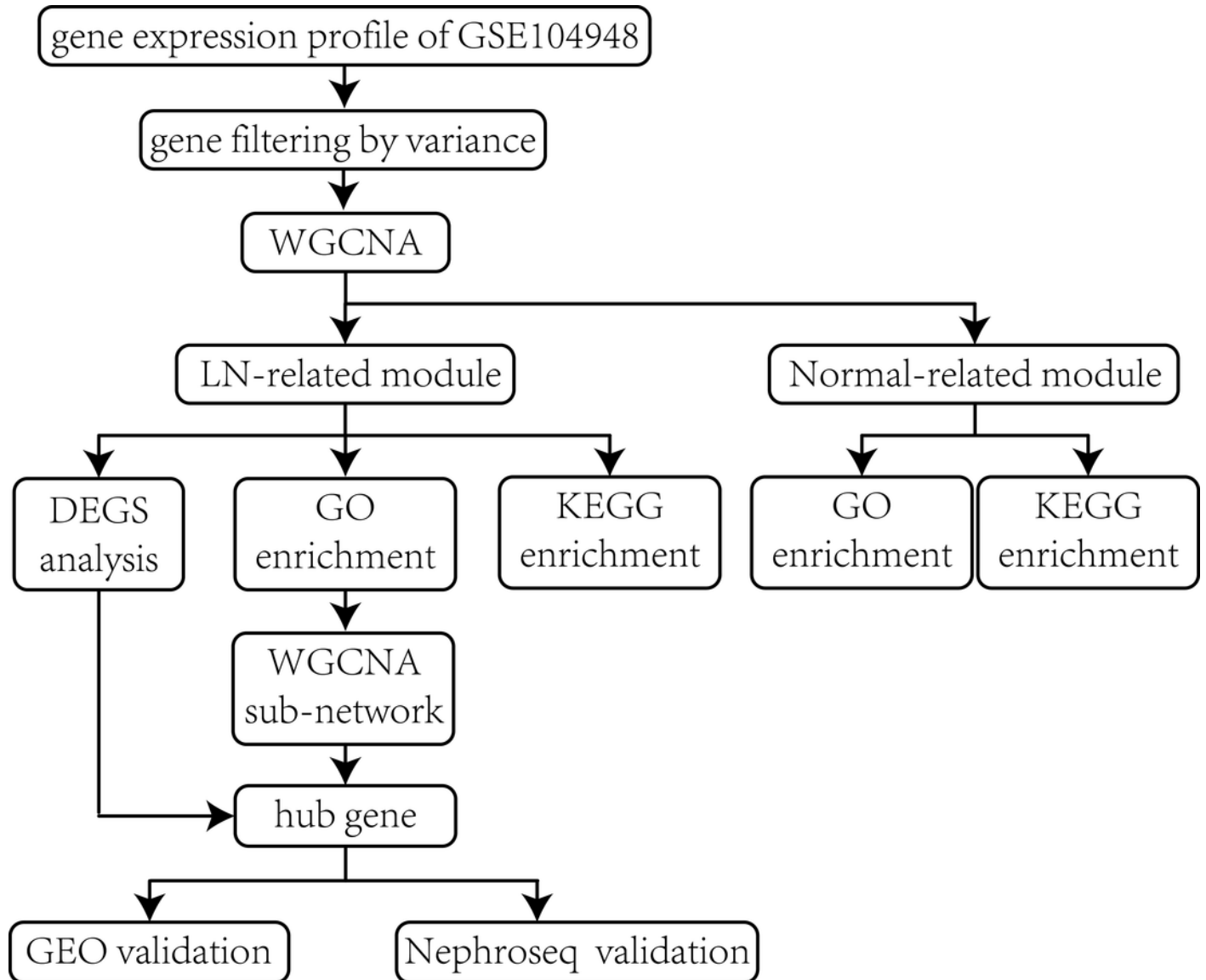


## Figure 2

Sample cluster dendrogram and soft-thresholding values ( $\beta$ ) estimation.

(A) Sample cluster dendrogram and clinical trait heatmap of 18 normal samples and 21 LN samples based on their expression profile. (B) Analysis of scale-free fit index of each  $\beta$  value from 1 to 30. (C) Analysis of mean connectivity of each  $\beta$  value from 1 to 30.  $\beta = 10$  was chosen for subsequent analyses as it has the biggest mean connectivity when the scale-free fit index is up to 0.85.

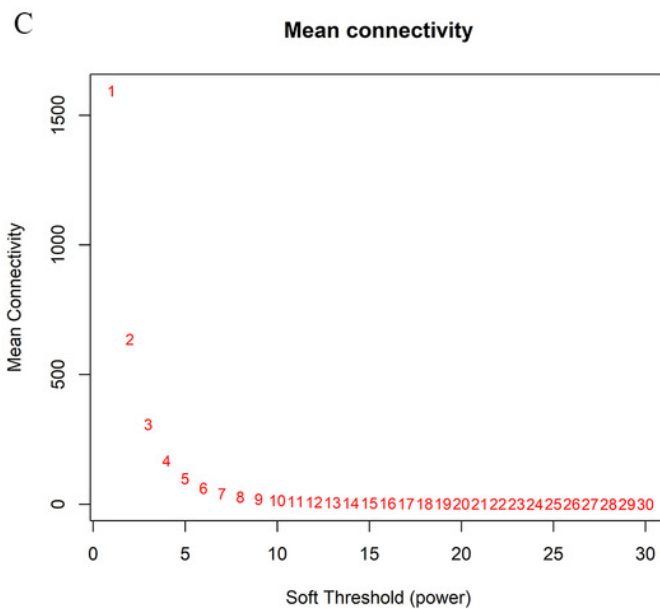
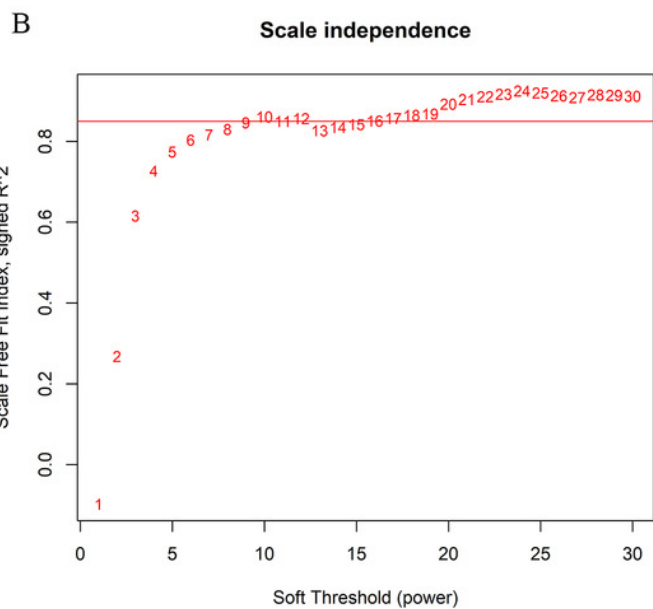
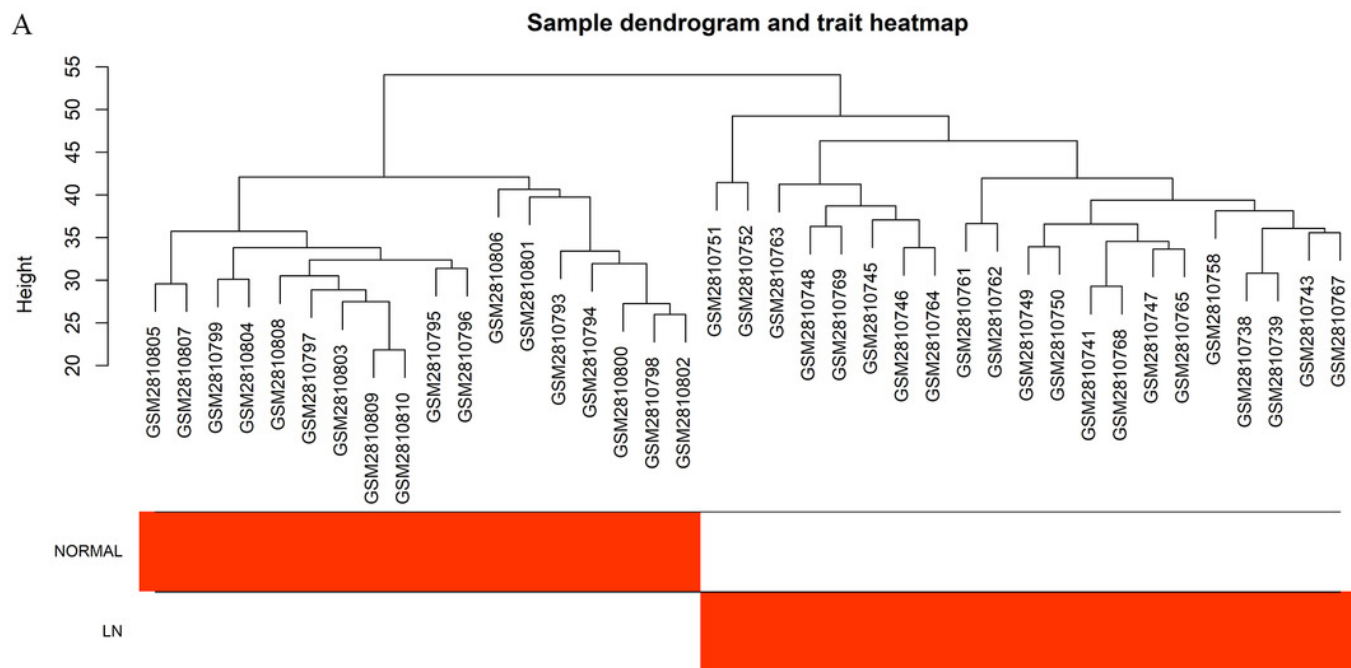


## Figure 3

Division and validation of co-expression modules.

(A) Dendrogram of all genes divided into 6 modules based on a dissimilarity measure (1-TOM). The modules labeled by color are indicated below the dendrogram. The upper part presents the original division by average linkage hierarchical clustering according to the TOM-based dissimilarity measure and the lower part presents the modules merged according to the Pearson's correlation of eigengenes. (B) Adjacency heatmap of the 5,942 genes analyzed by WGCNA. The depth of the red color indicates the correlation between all pair-wise genes. The red color mainly distributes in the diagonal of the heatmap. (C) Clustering dendrogram of eigengenes. (D) Adjacency heatmap of eigengenes. Red represented high adjacency (positive correlation) and blue represented low adjacency (negative correlation).

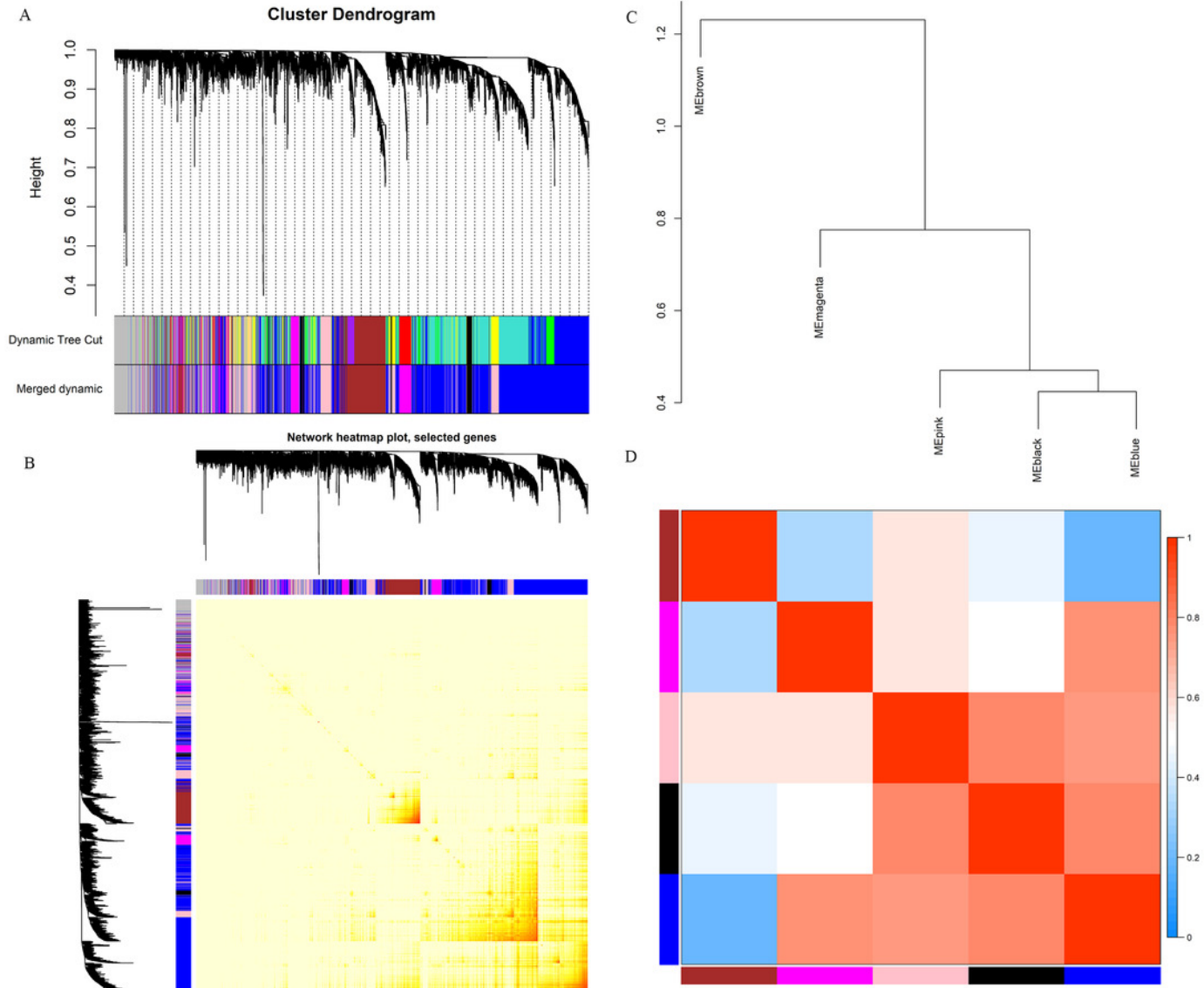


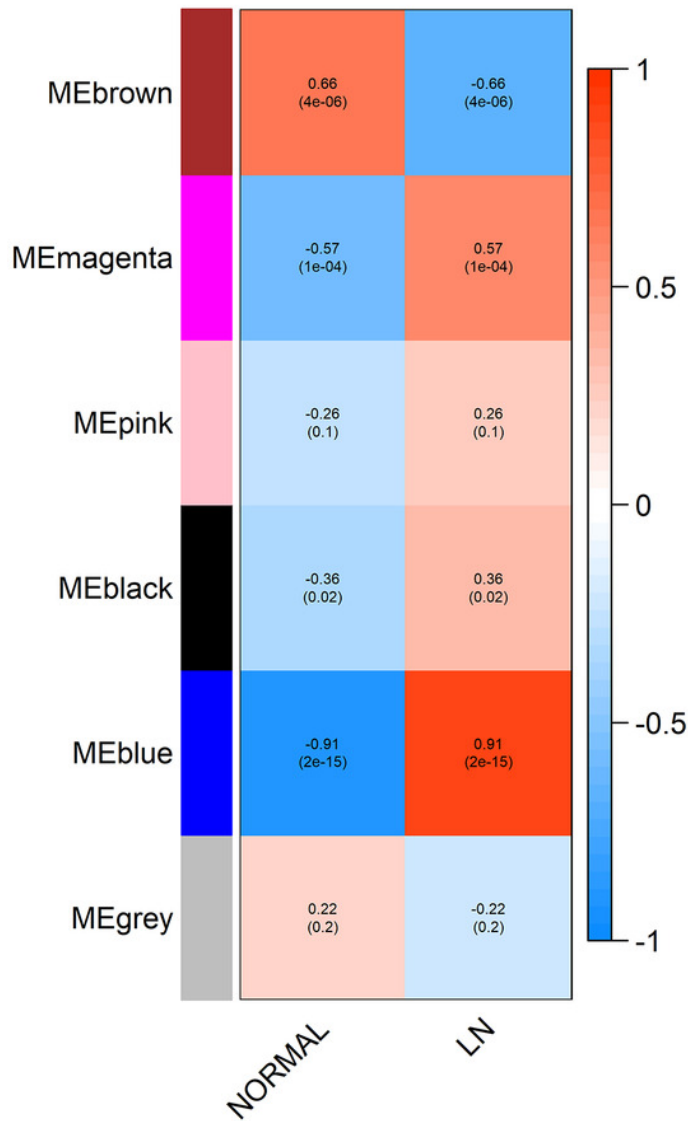
## Figure 4

Identification and verification of clinical related modules.

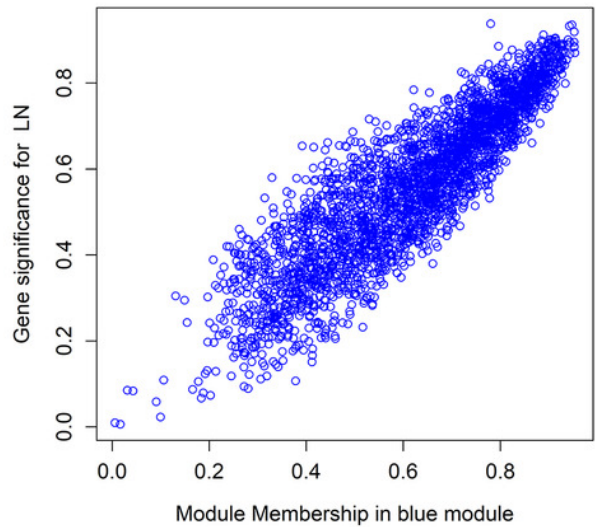
(A) Heatmap of module-trait correlations. Each cell depicts the correlation coefficients and  $P$ -value. The cells are colored by the intensity of correlation according to the color legend (red for positive correlation and blue for negative correlation). The blue module (top LN module) and brown module (top non-LN module) were identified as trait-related modules. (B) Scatter plot for correlation between the Gene significance (GS) and Module Membership (MM) in the top LN module. Correlation coefficients and  $P$ -value is labeled at the top. (C) Scatter plot for correlation between the GS and MM in the top non-LN module.

A

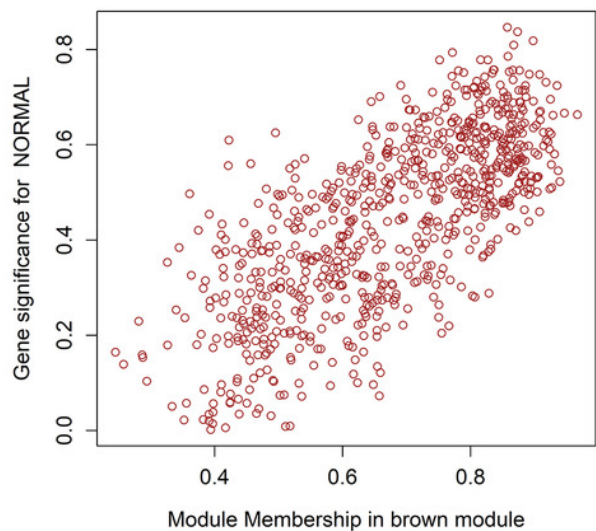
## Module-trait relationships



B

Module membership vs. gene significance  
cor=0.89, p<1e-200

C

Module membership vs. gene significance  
cor=0.73, p=3.1e-130

## Figure 5

DEGs analysis of two trait-related modules.

The color of each cell represents the expression level of a gene in a sample (red for high level and blue for low level). Only DEGs with top 30 logFC values are displayed. (A) Heatmap of DEGs in the top LN module. (B) Heatmap of DEGs in the top non-LN module.

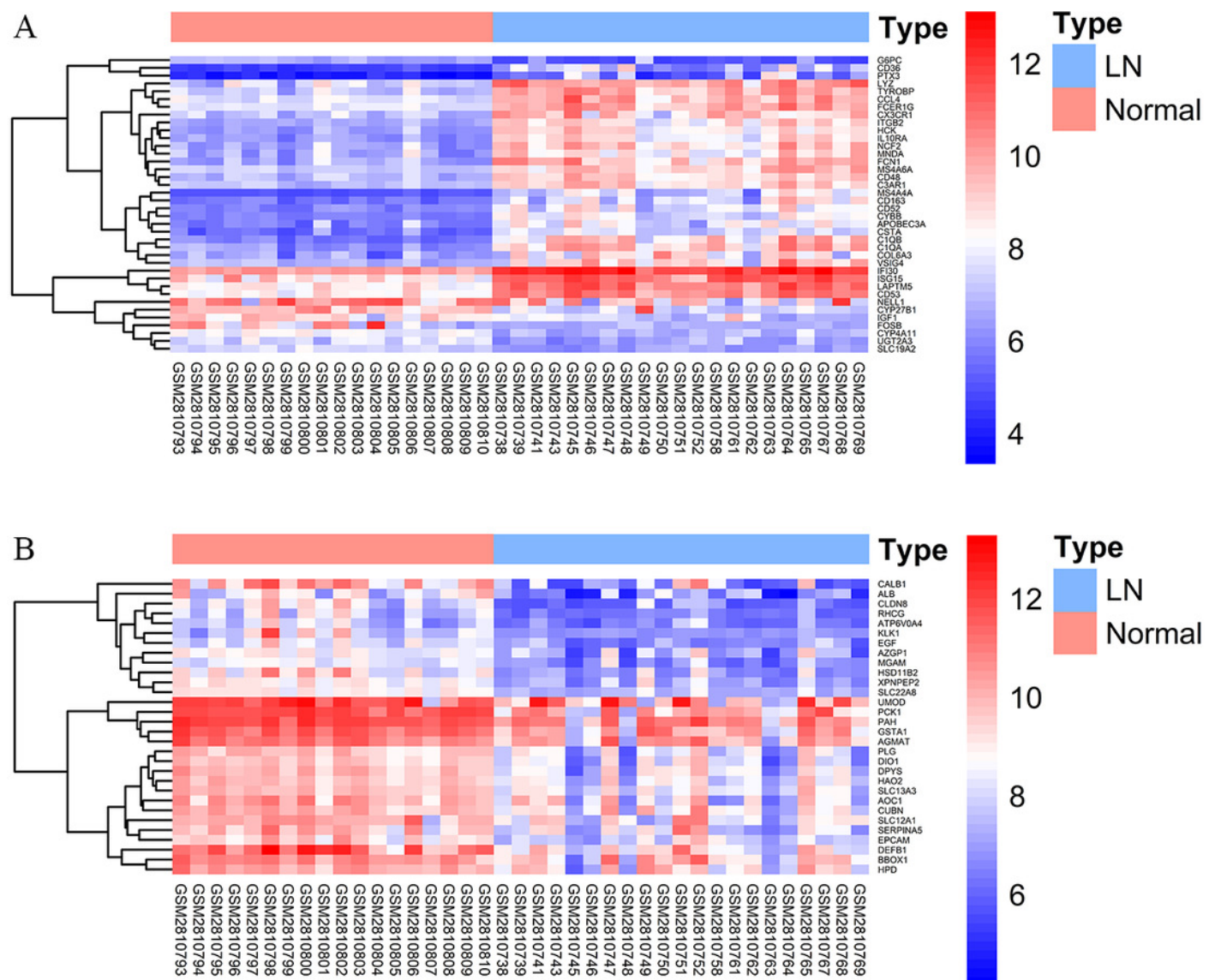


## Figure 6

GO enrichment analyses of two trait-related modules.

The depth of color is corresponded to the enrichment significant of each term and the x-axis indicates the enriched gene count. (A) Top 10 significantly enriched GO Biological Process (BP) terms of top LN module. (B) Top 10 significantly enriched GO Molecular Function (MF) terms of top LN module. (C) Top 10 significantly enriched GO Cellular Component (CC) terms of top LN module. (D) Top 10 significantly enriched GO Biological Process (BP) terms of top non-LN module. (E) Top 10 significantly enriched GO Molecular Function (MF) terms of top non-LN module. (F) Top 10 significantly enriched GO Cellular Component (CC) terms of top non-LN module.

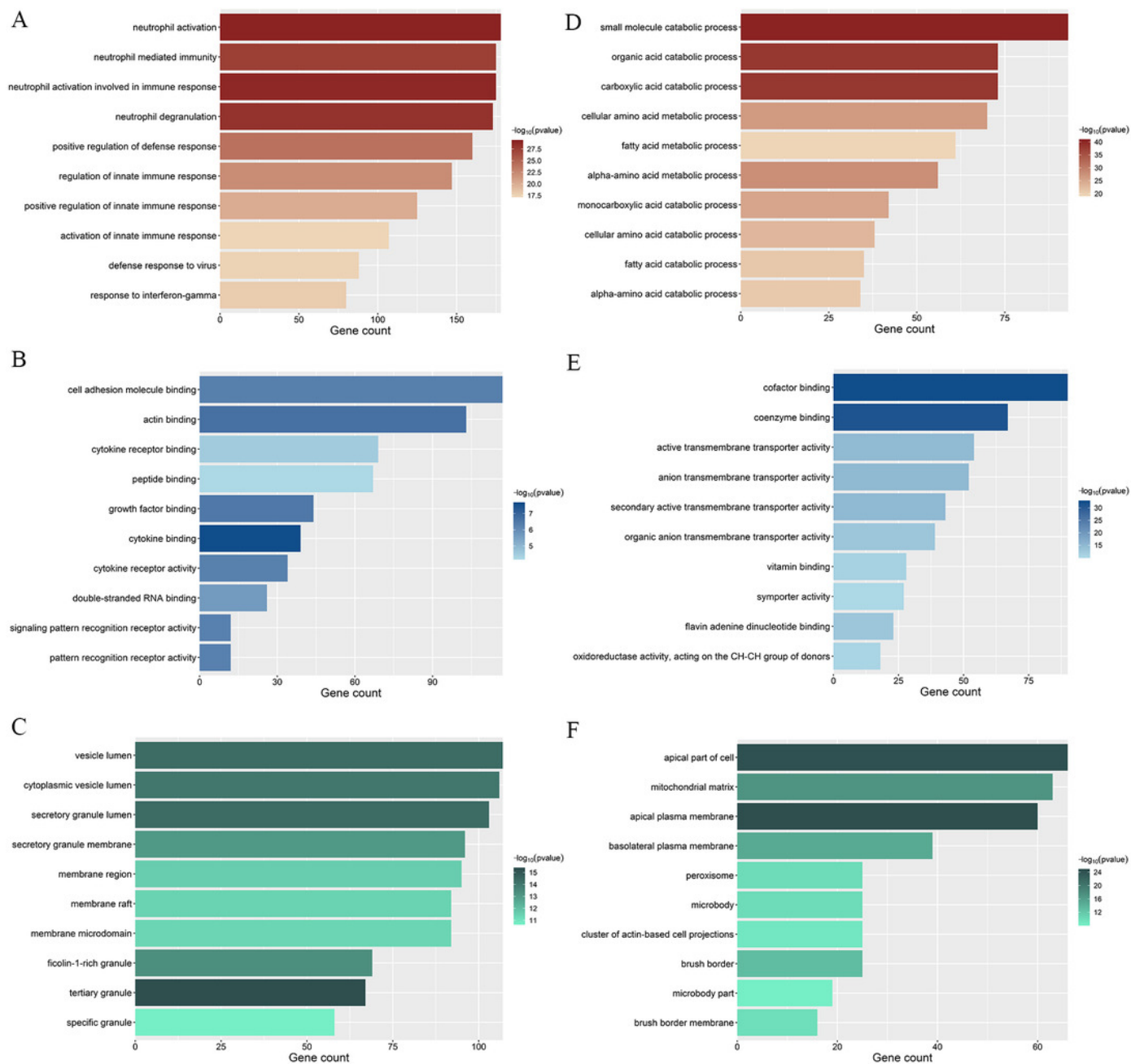


## Figure 7

KEGG enrichment analyses of two trait-related modules.

The depth of color is corresponded to the enrichment significant of each term and the size of the circle indicates the enriched gene count. (A) Top 10 significantly enriched KEGG terms of top LN module. (B) Top 10 significantly enriched KEGG terms of top non-LN module.

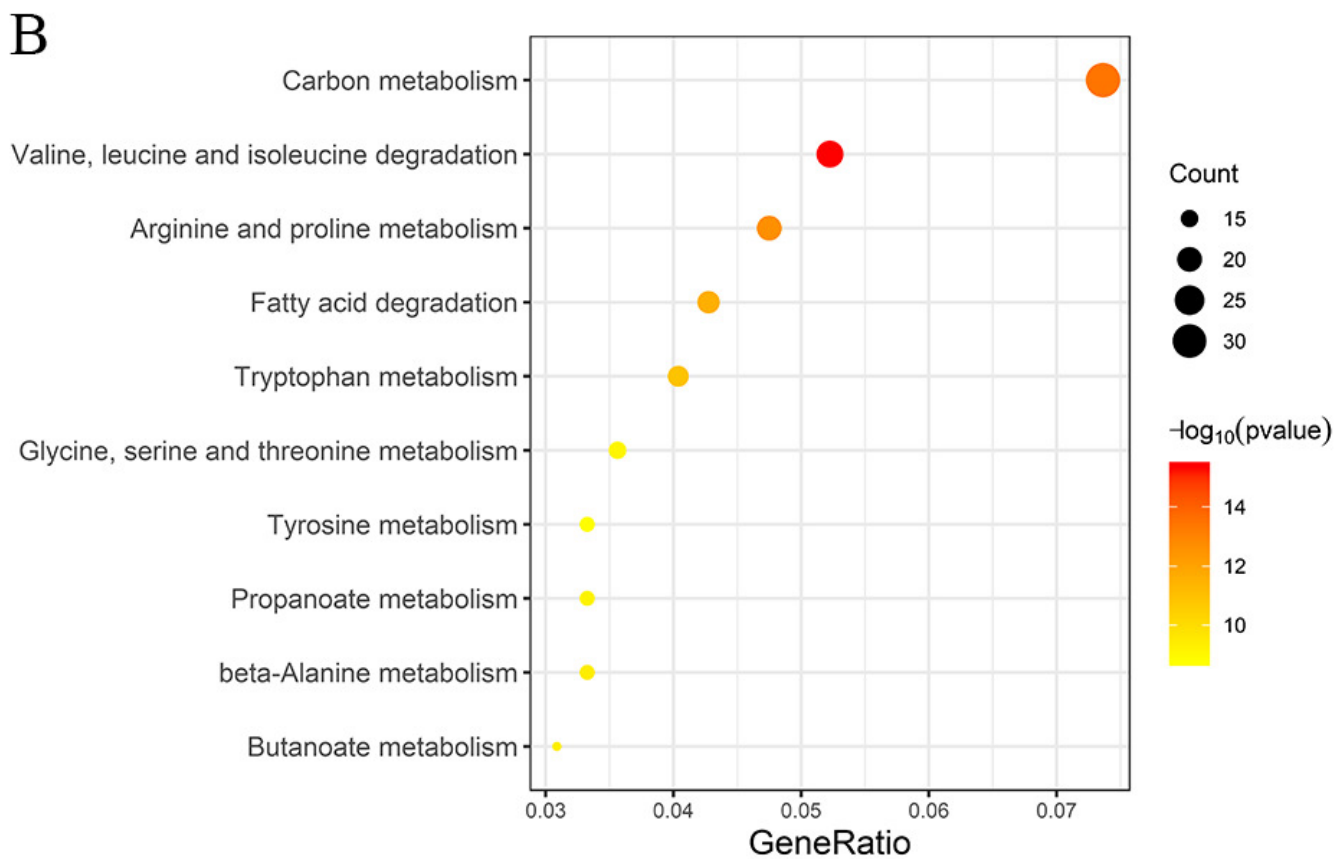
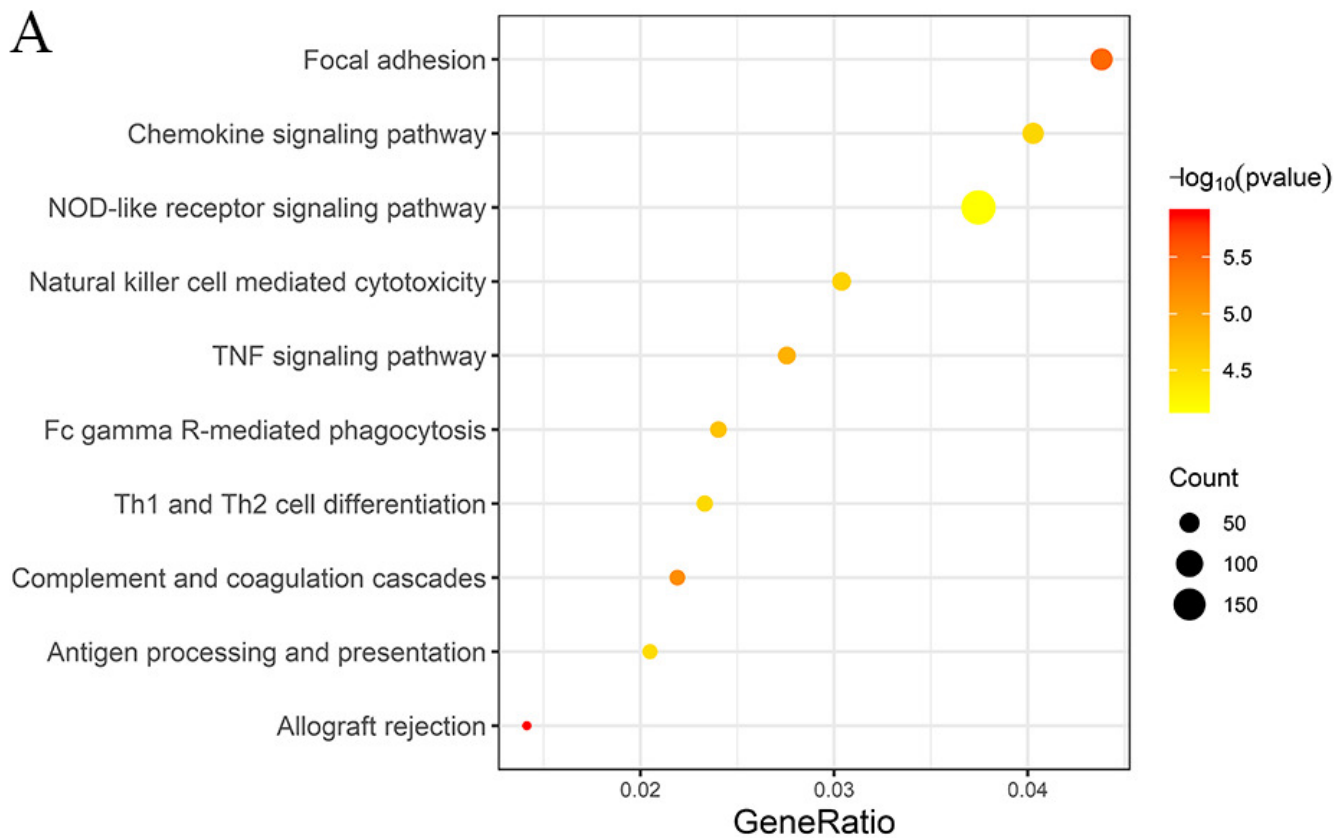


## Figure 8

Sub-networks of WGCNA based extracted based on most significant GO terms.

The nodes represent the genes and the edges represent the weighted correlation. Only co-expression pairs with top 500 weighted correlations are included. The red and yellow nodes represent genes of top 10 MCC values (red for a higher MCC value and yellow for lower). (A) Sub-network of the GO term “neutrophil activation”. (B) Sub-network of the GO term “positive regulation of defense response”.

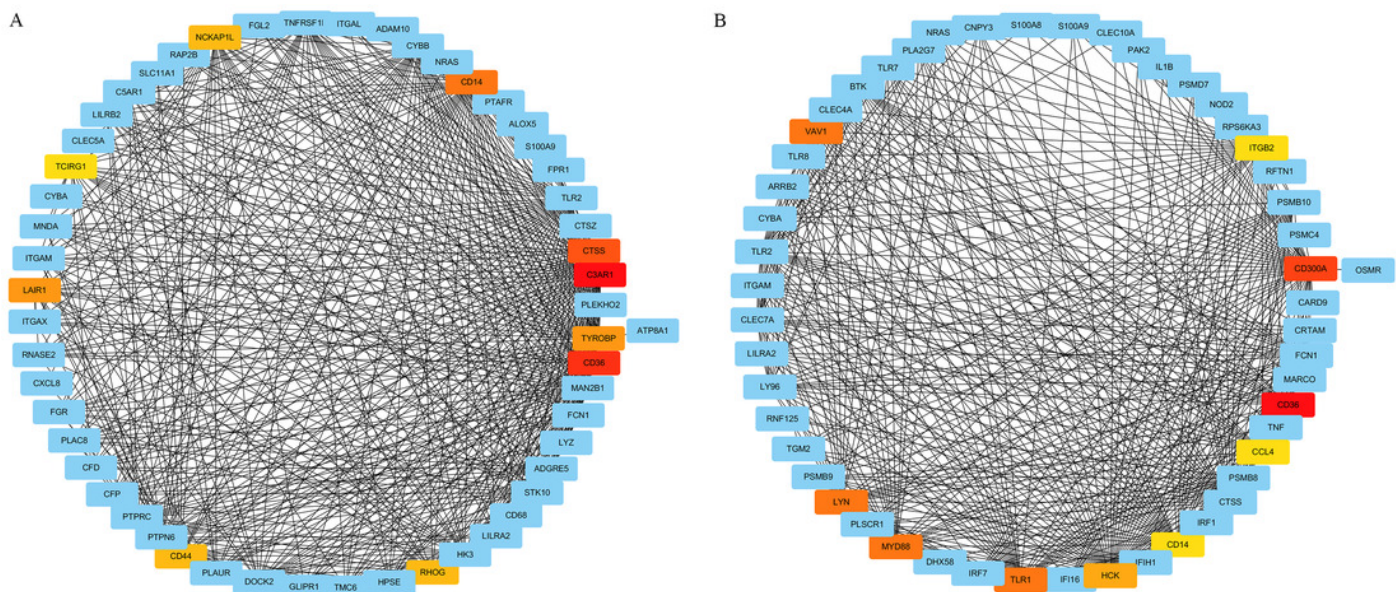


## Figure 9

Differentially expressed level of *CD36* between LN and normal in different GEO datasets.

(A) Expression level of *CD36* in dataset of GSE104948. (B) Expression level of *CD36* in dataset of GSE32591. (C) Expression level of *CD36* in dataset of GSE99339. (D) Expression level of *CD36* in dataset of GSE113342.

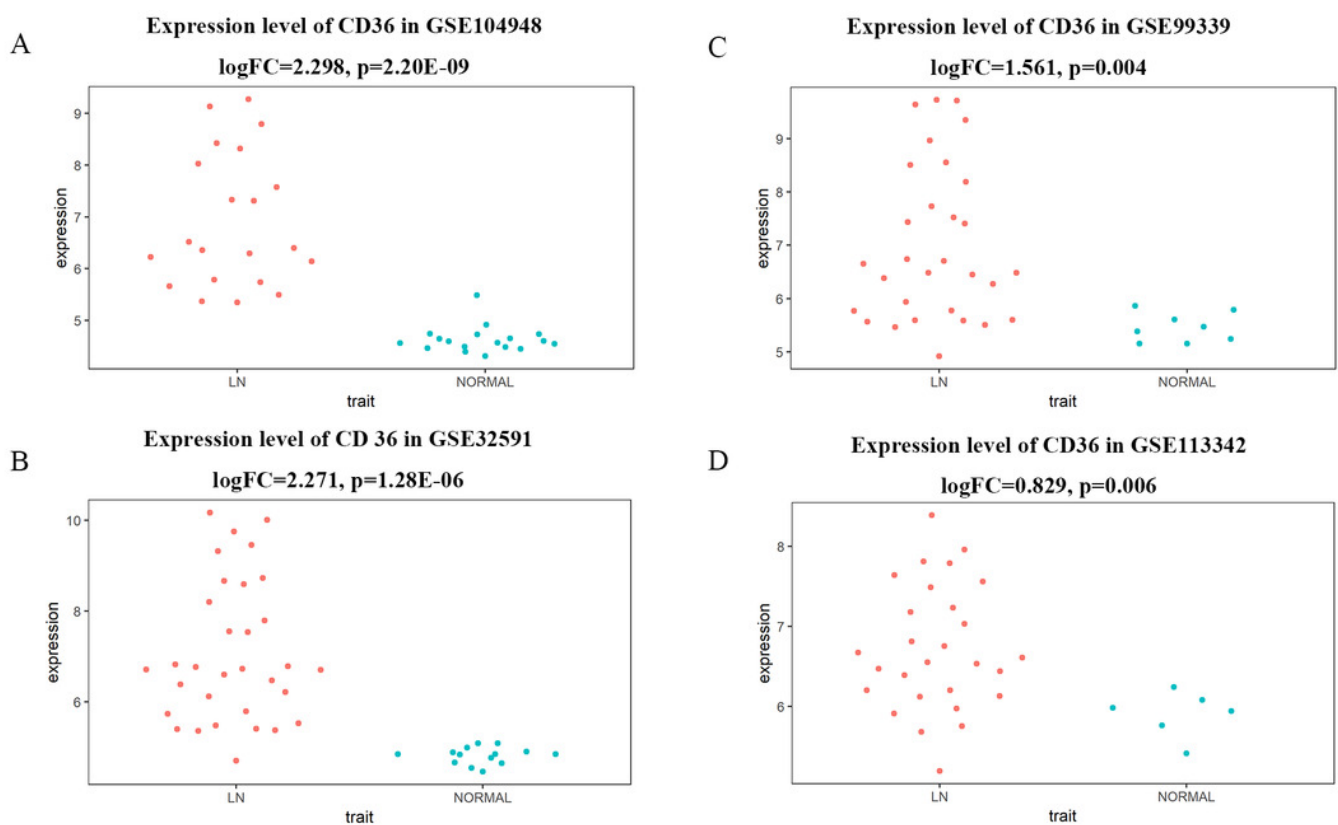


## Figure 10

Differentially expressed level of *CD36* in glomerular tissues of different WHO Lupus Nephritis Class.

(A) Differentially expressed level of *CD36* in class II and class IV respectively. (B) Differentially expressed level of *CD36* in class III and class IV respectively.

